

Phthalazinones 2: Optimisation and synthesis of novel potent inhibitors of poly(ADP-ribose)polymerase

Xiao-ling Cockcroft,^{a,*} Krystyna J. Dillon,^a Lesley Dixon,^b Jan Drzewiecki,^a
Frank Kerrigan,^b Vincent M. Loh, Jr.,^a Niall M. B. Martin,^a
Keith A. Menear^{a,*} and Graeme C. M. Smith^a

^a*KuDOS Pharmaceuticals Ltd 327 Cambridge Science Park, Milton Road, Cambridge, CB4 0WG, UK*

^b*Maybridge, Trevillet, Tintagel, Cornwall, PL34 0HW, UK*

Received 5 October 2005; revised 19 October 2005; accepted 22 October 2005

Available online 15 November 2005

Abstract—We have previously described the discovery of poly(ADP-ribose)polymerase-1 (PARP-1) inhibitors based on a phthalazinone scaffold. Subsequent optimisation of inhibitory activity, metabolic stability and pharmacokinetic parameters has led to a novel series of *meta*-substituted 4-benzyl-2*H*-phthalazin-1-one PARP-1 inhibitors which retain low nM cellular activity and show good stability in vivo and efficacy in cell based models.

© 2005 Elsevier Ltd. All rights reserved.

Poly(ADP-ribose)polymerase-1 (PARP-1) is an abundant nuclear enzyme that binds to and is activated by DNA single and double strand breaks. PARP-1 activation represents one of the earliest cell responses to DNA damage leading to DNA repair via the base-excision repair (BER) pathway.¹ Utilising nicotinamide adenine dinucleotide (NAD⁺) as substrate, PARP-1 catalyses the formation of ADP-ribose homopolymers onto PARP-1 and other protein acceptors. Due to its central role in a number of cellular processes PARP-1 has been implicated in several important disease states including cerebro-vascular disease, reperfusion injury and cancer resistance.^{2,3}

In tumour biology inhibition of PARP-1 activity has been shown to enhance the effects of radiation and chemotherapeutic agents by suppressing the repair of potentially lethal damage in cancerous cells.⁴ More recent studies have indicated that in certain genetic backgrounds tumour cells may be sensitive to the effects of PARP inhibition without the need for the presence of cytotoxic chemotherapeutics.^{5,6} For example, cells that showed loss of BRCA1 and BRCA2, components of

the homologous recombination DNA repair pathway, were seen to be extremely sensitive to the effects of PARP inhibition, leading to selective cell death.^{5,6}

These results indicate that for cancer treatment PARP inhibitors, whether as agents for combination with

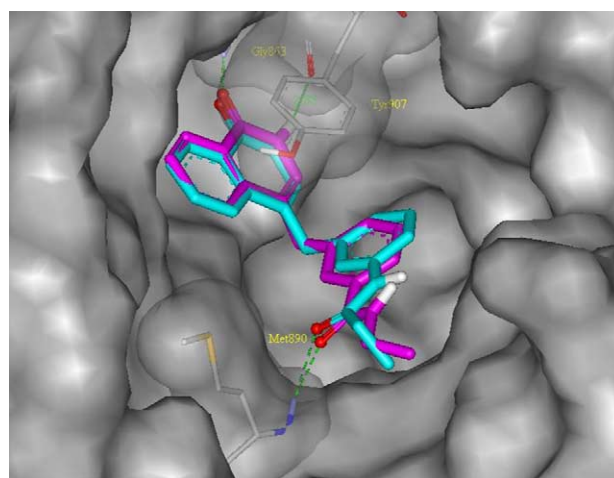
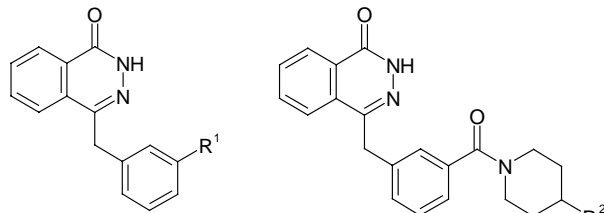


Figure 1. The overlay of the proposed docking model of compound 1 and 2 (shown in cyan and magenta, respectively) in the catalytic site of PARP-1. The protein is shown as a solid surface with Gly863, Met890 and Tyr907 through a transparent surface. Key hydrogen bonding interactions are indicated by green dotted lines.

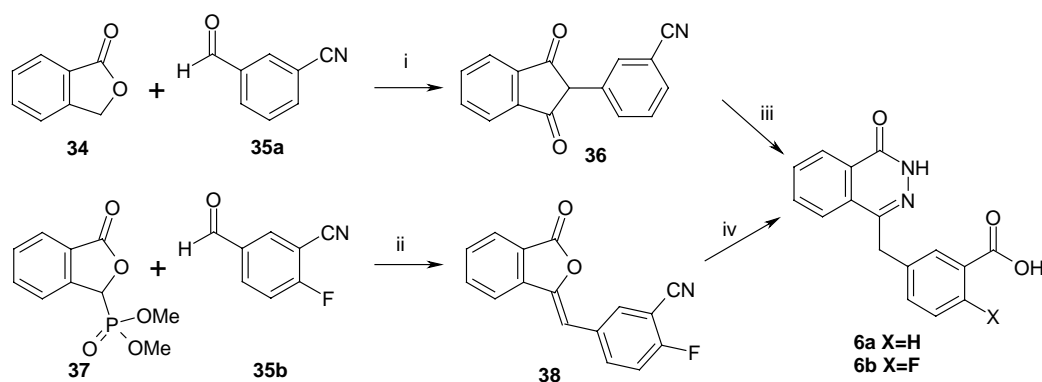
Keywords: PARP-1 inhibitor; Phthalazinone; DNA repair; Anti-cancer; BRCA2-deficient cell.

* Corresponding authors. Tel.: +44 1403 248844; e-mail addresses: xcockcroft@kudospharma.co.uk; kmenear@kudospharma.co.uk

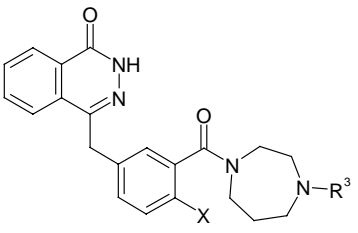
Table 1. Structure–activity relationships of the *meta*-substituted 4-benzyl-2*H*-phthalazin-1-one and the isonipecotate series


	R ¹	IC ₅₀ (nM)	PF ₅₀ ^a		R ²	IC ₅₀ (nM)	PF ₅₀
1		20	2.3	9		9	2.1
2		50	2.1	10		8	4.4
3		46	2.2	11		15	2.5
4		40	1.2	12		8	2.8
5		8	3.4	13		16	4.1
6		15	2.1	14		15	3.9
7		9	2.4	15		9	2.6
8		16	3.7	16		16	2.0

^a The PF₅₀ value is the potentiation factor, calculated as the ratio of the IC₅₀ growth curve for the alkylating agent, methyl methanesulfonate (MMS) divided by the IC₅₀ of the curve of MMS + PARP inhibitor.



Scheme 1. Synthesis route for phthalazinone acid intermediates. Reagents and conditions: (i) NaOCH₃, CH₃OH, reflux; (ii) NEt₃, THF; (iii) NH₂NH₂·H₂O, reflux; (iv) a—aq NaOH, THF; b—NH₂NH₂·H₂O, reflux.

Table 2. Structure–activity relationships of the homopiperazine series


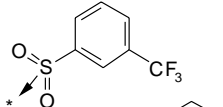
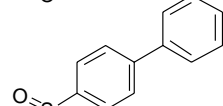
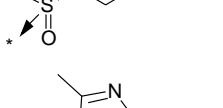
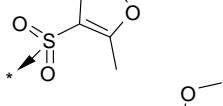
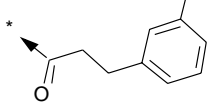
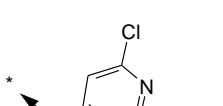
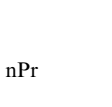
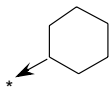
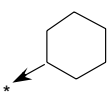
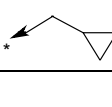
Compound	R ³	X	IC ₅₀ (nM)	PF ₅₀
17		H	8	2.1
18		H	6	3.2
19		H	12	2.1
20		H	8	2.5
21		H	9	2.5
22		H	8	2.2
7	H	H	9	2.4
23	Me	H	23	1.8
24	Et	H	15	2.6
25	nPr	H	10	2.5
26		H	6	6.6
27		H	14	3.1
28	H	F	7	12.6
29	Me	F	9	5.5

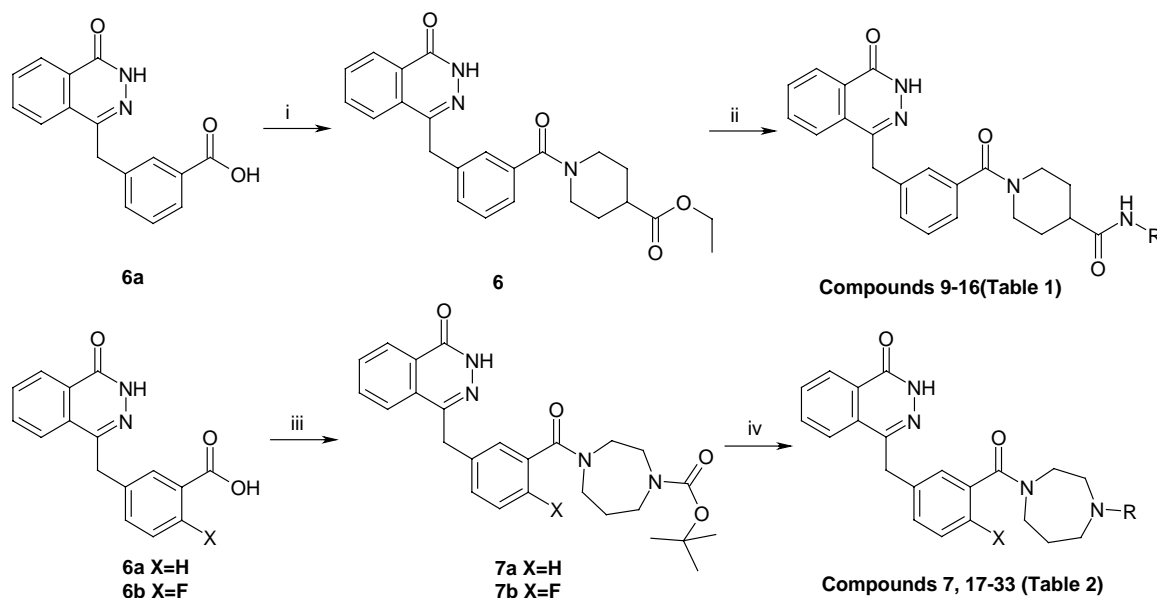
Table 2 (continued)

Compound	R ³	X	IC ₅₀ (nM)	PF ₅₀
30	Et	F	7	6.7
31	nPr	F	5	7.0
32		F	5	6.3
33		F	5	6.7

chemotherapies or as potential monotherapies, could be of significant therapeutic importance.

We have recently reported⁷ phthalazinone compound **1** (Table 1) as a potent inhibitor of PARP-1 with an IC₅₀⁸ of 20 nM and a cellular PF₅₀ ratio of 2.3. However, compound **1** was metabolised rapidly in vitro in mouse hepatic microsomes with an intrinsic clearance of 12 ml/min/g.

It was postulated that the pendant anilide at the *meta*-benzyl position was the most likely point of metabolic instability. Reversal of the anilide moiety in **1** to give amide **2** was predicted to retain activity whilst improving metabolic stability. Docking of **1** and **2** into the known crystal structure of chicken PARP-1, PDB code, *Ipax*,⁹ utilising Monte-Carlo (MacroModel version 7.1)¹¹ provides a proposed binding mode for the compounds (Fig. 1). The phthalazinone ring of **1** and **2** forms a hydrophobic π - π stacking interaction with the phenyl moiety of Tyr907. The amido NH and carbonyl of the phthalazinone ring on both **1** and **2** interact identically with the backbone carbonyl and NH of Gly863 through bidentate hydrogen bonding, characteristic of this class of inhibitors.^{9,10,12} The binding model of the amide and anilide carbonyl on the *meta*-benzyl position of **1** and **2** predicts a hydrogen bonding interaction with the backbone NH of Met890, possibly replacing a conserved water molecule identified in the crystal structure of PARP-1. Indeed, compound **2** gave similar PARP-1 inhibition but with a considerably enhanced metabolic stability in vitro in mouse hepatic microsomes, with an intrinsic clearance less than 1 ml/min/g. Based on these observations a diverse library of amides was synthesized to explore the SAR further. The synthesis was carried out using parallel synthesis methodologies by employing the phthalazinone acid **6a** (Scheme 1) as the key functional intermediate. Preliminary structure–activity exploration showed that a wide range of amines could be accommodated in this region without losing potency against the enzyme. More significantly, a number of compounds from this library showed comparable or improved cellular activity over and above compound **1**, exemplified by entries **1–18** in Table 1. Two further complementary libraries were subsequently designed and synthesized. The first library (**9–16**) utilised the free acid of **6** coupled to a diverse set of amines. The second library (**17–22**, Table 2) further exploited



Scheme 2. Synthesis route for phthalazinone nipecotate and homopiperazine analogues. Reagents and conditions: (i) HBTU, ethyl nipecotate, Hunigs base, DCM; (ii) a—2 M NaOH, THF; b—HBTU, DMA, RHN₂; (iii) HBTU, *tert*-butyl homopiperazine-1-carboxylate, Hunigs base, DMA; (iv) a—6 M HCl, EtOH; b—RCOCl or RSO₂Cl or RNCO, Hunigs base, DCM or RCHO, NaBH(CH₃CO₂)₃, acetic acid, DCM.

7 through coupling with alkyl, acyl, sulfonyl or urea groups. The SAR developed from these compounds illustrates that a wide variety of substituents can be tolerated at the terminal position of the molecule. This observation can be rationalised if these side chains are approaching the solvent surface (Fig. 1) and do not significantly interact with the enzyme. However, it was noted that hydrophobic residues are preferred at this position particularly if cellular activity is to be maintained. Of note is the overall enhancement of PF₅₀ values, with compound 10 being the most attractive in the series with a PF₅₀ value of 4.1. Alkylation of the homopiperazine template 7 provided a series of compounds (23–27, Table 2), which exhibit good IC₅₀ and PF₅₀ values. Further introduction of fluorine at the *para* position of the pendant benzene ring, aiming to block possible metabolism at this position and extend half life, resulted in a class of potent inhibitors with excellent cellular activity (28–33, Table 2). Whilst potency at the enzyme was maintained with compounds 28–33, the PF₅₀ values were significantly increased. In nearly every case, introduction of a fluorine at this *para* position leads to more than a doubling of the PF₅₀ value vis-à-vis the des-fluoro analogues.

Compound 28 was further characterised in an *in vivo* pharmacokinetic model (rat, 10 mg/kg, iv) where it demonstrated a *T*_{1/2} of 60 min, clearance 54 ml/min/kg and a volume of distribution of 2.1 L/kg. The aqueous solubility of compound 28 at pH 7.4 buffer was 5.1 mg/ml. Notably, 28 is exquisitely potent in specific killing of cells defective in the tumour suppressor genes BRCA1 or BRCA2. The SF₅₀ (dosage at which 50% of cell survived) of 28 is 15 nM for BRCA2-deficient cells and 2 μM for wild type cells.⁶

The synthesis of the key intermediate phthalazinone acids 6a and 6b is outlined in Scheme 1. For the des-fluoro analogue (6a, X = H) simple nucleophilic addition of phthalide 34 to the aldehyde 35a in the presence of sodium methoxide, followed by nitrile hydrolysis and cyclisation of the indanedione 36 with hydrazine hydrate, gave 6a. For fluoro analogue 6b, in which the fluoro *ortho* to the nitrile group is labile to nucleophilic displacement, the alternative milder route via phosphonate 37 was required.

The nipecotate (9–16) and homopiperazine (7, 17–33) analogues were synthesized in parallel from intermediates 6a or 6b using the two-step process as outlined in Scheme 2.

In conclusion, the optimization, synthesis and preliminary biological evaluation of a novel class of phthalazinones as potent and cellularly active PARP-1 inhibitors have been described. In particular, compound 28 has been characterised as a compound having attractive pharmacokinetic and physicochemical properties for iv administration. Further evaluation of this class of compounds is ongoing and will be reported in due course.

References and notes

- Satoh, M.; Lindahl, T. *Nature* **1992**, 356, 356.
- Szabo, S.; Zingarelli, B.; O'Connor, M.; Salzman, A. L. *J. Clin. Invest.* **1997**, 100, 723.
- Cantoni, O.; Cattbeni, F.; Stocchi, V.; Meyn, R. E.; Cerrutti, P.; Murray, D. *Biochem. Biophys. Acta* **1989**, 1014, 1.
- Curtin, N. J. *Expert Rev. Mol. Med.* **2005**, 7, 1.

5. Bryant, H. E.; Schultz, N.; Thomas, H. D.; Parker, K. M.; Flower, D.; Lopez, E.; Kyle, S.; Meouth, M.; Curtin, N. J.; Helleday, T. *Nature* **2005**, *434*, 913.
6. Farmer, H.; McCabe, N.; Lord, C. J.; Tutt, A. N. J.; Johnson, D. A.; Richardson, T. B.; Santarosa, M.; Dillon, K. J.; Hickson, I.; Knights, C.; Martin, N. M. B.; Jackson, S. P.; Smith, G. C. M.; Ashworth, A. *Nature* **2005**, *434*, 917.
7. Loh, V. M.; Cockcroft, X.; Dillon, K. J.; Dixon, L.; Drzewiecki, J.; Eversley, P. J.; Gomez, S.; Hoare, J.; Kerrigan, F.; Matthews, I. T. W.; Menear, K. A.; Martin, N. M. B.; Newton, R. F.; Paul, J.; Smith, G. C. M.; Vile, J.; Whittle, A. J. *Bioorg. Med. Chem. Lett.* **2005**, *15*, 2235.
8. Dillon, K. J.; Smith, G. S.; Martin, N. M. B. *J. Biomol. Screen.* **2003**, *8*, 347.
9. Ruf, A.; de Murcia, J. M.; de Murcia, G.; Schulz, G. E. *Proc. Natl. Acad. Sci. U.S.A.* **1996**, *93*, 7481.
10. Ruf, A.; de Murcia, G.; Schulz, G. E. *Biochemistry* **1998**, *37*, 3893.
11. MacroModel version 7.1, Schrödinger Inc. 1999–2000.;
12. White, A. W.; Almsy, R.; Calvert, H. A.; Curtin, N. J.; Griffin, R. J.; Hostomsky, Z.; Maegley, K.; Newell, D. R.; Golding, B. T. *J. Med. Chem.* **2000**, *43*, 4084.